*Int. J. Exp. Path.* (2010), 91, 54–62
doi: 10.1111/j.1365-2613.2009.00683.x

ORIGINAL ARTICLE

# Myostatin and follistatin expression in skeletal muscles of rats with chronic heart failure

Aline Regina Ruiz Lima*, Paula Felippe Martinez*, Katashi Okoshi*, Daniele Mendes Guizoni*, Leonardo A. Mamede Zornoff*, Dijon Henrique Salomé Campos*, Sílvio Assis Oliveira Jr *, Camila Bonomo*, Maeli Dal Pai-Silva† and Marina Politi Okoshi*

*Department of Internal Medicine, Botucatu Medical School, State University of Sao Paulo – UNESP, Botucatu, Sao Paulo, Brazil and †Department of Morphology, Botucatu Biosciences Institute, State University of Sao Paulo – UNESP, Botucatu, Sao Paulo, Brazil

INTERNATIONAL JOURNAL OF EXPERIMENTAL PATHOLOGY

## Summary

Skeletal muscle abnormalities can contribute to decreased exercise capacity in heart failure. Although muscle atrophy is a common alteration in heart failure, the mechanisms responsible for muscle mass reduction are not clear. Myostatin, a member of TGF-β family (transforming growth factor), regulates muscle growth and mass. Several studies have shown a negative correlation between myostatin expression and muscle mass. The aim of this study was to evaluate myostatin expression in skeletal muscles of rats with heart failure. As myostatin gene expression can be modulated by follistatin, we also evaluated its expression. Heart failure was induced by myocardial infarction (MI, $n = 10$); results were compared to Sham-operated group ($n = 10$). Ventricular function was assessed by echocardiogram. Gene expression was analyzed by real-time PCR and protein levels by Western blotting in the soleus and gastrocnemius muscles; fibre trophism was evaluated by morphometric analysis. MI group presented heart failure evidence such as pleural effusion and right ventricular hypertrophy. Left ventricular dilation and dysfunction were observed in MI group. In the soleus muscle, cross-sectional area ($P = 0.006$) and follistatin protein levels (Sham 1.00 ± 0.36; MI 0.18 ± 0.06 arbitrary units; $P = 0.03$) were lower in MI and there was a trend for follistatin gene expression to be lower in MI group ($P = 0.085$). There was no change in myostatin expression between groups. In gastrocnemius, all MI group parameters were statistically similar to the Sham. In conclusion, our data show that during chronic heart failure, decreased skeletal muscle trophism is combined with unchanged myostatin and reduced follistatin expression.

**Keywords**
cardiac failure, follistatin, myocardial infarction, myostatin, PCR, skeletal muscle

Received for publication:
27 June 2009
Accepted for publication:
17 August 2009

**Correspondence:**
Marina Politi Okoshi
Departamento de Clinica Medica
Faculdade de Medicina de Botucatu,
UNESP, Rubiao Junior, S/N
CEP: 18618-000 – Botucatu Sao Paulo
Brazil
Tel.: +55 14 3811 6213
Fax: +55 14 3882 2238
E-mail: mpoliti@fmb.unesp.br

Heart failure is characterized by a decreased exercise capacity due to the early appearance of symptoms like dyspnoea and muscle fatigability. Although these symptoms can be caused by reduced cardiac output, there is no clear association between exercise intolerance and hemodynamic parameters (Mancini *et al.* 1992; Harrington *et al.* 2001). It has been suggested that intrinsic skeletal muscle abnormalities play a role in decreased exercise capacity and heart failure symptoms (Vescovo *et al.* 1998).

Muscle wasting is common in chronic illnesses such as those associated with HIV infection, some types of cancer, and heart failure (Mancini *et al.* 1992; Gonzalez-Cadavid *et al.* 1998; Bruera & Sweeney 2000). The mechanisms responsible for muscle atrophy in heart failure are not clear. Myostatin, a recently identified member of the transforming growth factor beta (TGF-β) superfamily of secreted growth and differentiation factors, regulates muscle growth, acting as a negative regulator of skeletal muscle mass (McPherron *et al.* 1997; Lee 2004). Several studies have shown a negative correlation between myostatin expression and muscle mass. Mutations of myostatin gene in cattle are associated with muscle hypertrophy (McPherron & Lee 1997). Similarly, myostatin-null mice present increased muscle mass, resulting from both muscle fibre hyperplasia and hyperthrophy (McPherron *et al.* 1997). Pharmacological treatment with a myostatin antibody increased skeletal muscle mass and grip strength (Whittemore *et al.* 2003). Furthermore, systemic overexpression of myostatin in adult mice was found to induce profound muscle and fat loss (Zimmers *et al.* 2002). In a clinical setting, recent investigations have suggested that myostatin may be involved in the muscle mass reduction observed in AIDS and cancer patients (Gonzalez-Cadavid *et al.* 1998; Acharyya & Gutttridge 2007). In HIV-infected men, increased levels of myostatin immunoreactive material in serum and skeletal muscle appear to correlate with the presence of cachexia (Gonzalez-Cadavid *et al.* 1998). In heart failure, the role of myostatin on skeletal muscle wasting remains unclear. Recently, Lenk *et al.* (2009) reported that myostatin was up-regulated in cardiac and skeletal muscle during experimental heart failure. The aim of this study was to evaluate myostatin mRNA and protein expression and skeletal muscle trophism in rats with myocardial infarction-induced heart failure. As myostatin expression can be modulated by follistatin, an antagonistic protein, we also evaluated follistatin expression.

## Materials and methods

### *Experimental groups*

All experiments and procedures were performed in line with the Guide for the Care and Use of Laboratory Animals published by the US National Institute of Health and were approved by the Ethics Committee of the Botucatu Medical School, UNESP, SP, Brazil.

Male Wistar rats (200–250 g) were purchased from the Central Animal House at the Botucatu Medical School, UNESP. Myocardial infarction was induced according to a previously described method (Zornoff *et al.* 2000). In summary, rats were anesthetized with ketamine (60 mg/kg) and submitted to left lateral thoracotomy ($n$ = 18). After heart exteriorization, the left atrium was retracted to facilitate left coronary artery ligation with 5–0 mononylon between the pulmonary outflow tract and the left atrium. The heart was then replaced in the thorax, the lungs inflated by positive pressure, and the thoracotomy closed. Sham-operated rats were used as controls ($n$ = 10). Five rats (28%) died within 24 h after surgery and two died during the follow-up period. All animals were housed in a temperature controlled room at 23 °C and kept on a 12-h light/dark cycles. Food and water were supplied *ad libitum*.

Three weeks after surgery, rats were subjected to transthoracic echocardiogram. Infarct size at midpapillary muscle level was estimated from 2D short-axis left ventricular (LV) images at end diastole and analysed as a percentage of the LV endocardial circumference (Ahmet *et al.* 2005). As our goal was to study rats with heart failure, animals with small or moderate infarcts were discarded from this study. Six months after inducing myocardial infarction, the rats were subjected to transthoracic echocardiography and killed the next day. At the time of euthanasia, we evaluated the presence of clinical and pathological evidence of heart failure. Clinical findings suggesting heart failure were tachypnea/dyspnoea. Pathologic assessment of cardiac decompensation included pleuropericardial effusion, atrial thrombi, and right ventricular hypertrophy (right ventricle weight-to-body weight ratio greater than 0.8 mg/g) (Bing *et al.* 1995; Brooks *et al.* 1997; Cicogna *et al.* 1999). The myocardial infarction group (MI) was composed of rats with right ventricular hypertrophy and at least one clinical and/or pathological evidence of heart failure (which comprised 8 out of 11 survival infarcted rats).

### *Echocardiographic study*

Rats were anesthetized with an intramuscular injection of ketamine (50 mg/kg) and xylazine (1 mg/kg). The chest was shaved and rats positioned on their left side. Using an echocardiograph (HDI 5000 SonoCT, Philips, Bothell, WA, USA) equipped with a 12 MHz transducer, a two-dimensional parasternal short-axis view of the left ventricle (LV) was obtained at the level of the papillary muscles. M-mode

 

tracings were obtained from short-axis views of the LV at or just below the tip of the mitral-valve leaflets, and at the level of the aortic valve and left atrium (Litwin *et al.* 1995; Okoshi *et al.* 2002; Paiva *et al.* 2003). M-mode images of LV were recorded on a black-and-white thermal printer (Sony UP-890MD, Tokyo, Japan) at a sweep speed of 100 mm/s. All LV tracings were manually measured by the same observer according to the leading-edge method of the American Society of Echocardiography (Sahn *et al.* 1978) which was validated for the infarcted rat model (Solomon *et al.* 1999). Measurements were the mean of at least five cardiac cycles on the M-mode tracings. The following structural variables were measured: left atrium dimension (LA), aorta dimension (AO), left ventricular diastolic and systolic dimension (LVDD and LVSD, respectively), and left ventricular diastolic posterior wall thickness (LVDPWT) and septal wall thickness (LVDSWT). Left ventricular function was assessed by the following parameters: heart rate (HR), endocardial fractional shortening (FS), posterior wall shortening velocity (PWSV), early and late diastolic mitral inflow (E-wave and A-wave, respectively), E/A ratio, E wave deceleration time (EDT), and isovolumetric relaxation time (IVRT).

### *Morphological analysis*

At the time of euthanasia, the animals were weighed and anesthetized with intraperitoneal sodium pentobarbital (50 mg/kg). Hearts were removed by thoracotomy and the atria and ventricles were separated and weighed. The soleus and superficial white portions of gastrocnemius muscles were dissected, weighed, immediately frozen in liquid nitrogen, and stored at −80 °C.

Infarct size was measured by left ventricle histological analysis in haematoxylin and eosin stained sections according to a previously described method (Minicucci *et al.* 2007). Infarction size was calculated by dividing endocardial and epicardial ventricular circumferences in the infarcted area by total endocardial and epicardial circumferences. Measurements were taken in cross-sectional planes of the left ventricle, 5–6 mm from the apex, assuming that the planes in this region present a linear relation with the sum of the measurements of the areas of all heart planes (Oh *et al.* 1993).

Transverse sections approximately 10 μm thick of the frozen soleus and gastrocnemius were cut in a cryostat at −20 °C and stained with haematoxylin and eosin. Muscle trophism was assessed by measuring at least 200 cross-sectional fibre areas from each muscle. Measurements were performed using a compound microscope LEICA DM LS attached to a computerized imaging analysis system (Media Cybernetics, Silver Spring, MD, USA).

### *Real time RT-PCR (transcription polymerase chain reaction after reverse transcription) analysis*

Total RNA was extracted from skeletal muscles with TRIzol Reagent (Invitrogen Life Technologies, Carlsbad, CA, USA) according to a previously described method (Lopes *et al.* 2008). Frozen muscles were mechanically homogenized on ice in 1 ml of ice-cold TRIzol reagent. Total RNA was solubilized in RNase-free $H_2O$, incubated in DNase I (Invitrogen Life Technologies) to remove any DNA in the sample, and quantified by measuring optical density (OD) at 260 nm. RNA purity was ensured by obtaining a 260/280 nm OD ratio of approximately 2.0. One microgram of RNA was reverse transcribed using High Capacity cDNA Reverse Transcription Kit in a total volume of 20 μl, according to standard methods (Applied Biosystems, Foster City, CA, USA). Aliquots of 2.5 μl (10–100 ng) of cDNA were then submitted to real-time PCR reaction using 10 μl 2X TaqMan® Universal PCR Master Mix (Applied Biosystems) and 1 μl of customized assay (20X) containing sense and antisense primers and Taqman (Applied Biosystems) probe specific to each gene, myostatin (Taqman assay Rn00569683_m1; Ref. seq. Genbank NM_019151.1) and follistatin (Taqman assay Rn00561225_m1; Ref. seq. Genbank NM_012561.1). The amplification and analysis were performed using Step One Plus™ Real Time PCR System (Applied Biosystems), according to the manufacturer's recommendation. Expression data were normalized to cyclophilin expression (reference gene; Taqman assay Rn00690933_m1; Ref. seq. Genbank NM_017101.1). Reactions were performed in triplicate and expression levels calculated using the $C_T$ comparative method ($2^{-\Delta\Delta CT}$).

### *Western blotting analysis*

Protein levels of soleus and gastrocnemius muscles were analyzed by Western Blot according to a method previously described (Costelli *et al.* 2008) with specific antibodies: anti-myostatin and anti-follistatin (GDF-8 N-19-R sc-6885-R and H-114 sc-30194, respectively, Santa Cruz Biotechnology, Santa Cruz, CA, USA). Protein levels were normalized to those of GAPDH (6C5 sc-32233, Santa Cruz Biotechnology. Muscle protein was extracted using Tris-Triton buffer (10 mM Tris pH 7.4, 100 mM NaCl, 1 mM EDTA, 1 mM EGTA, 1% Triton X-100, 10% glycerol, 0.1% SDS, 0.5% deoxycholate) and the protein content of supernatant was quantified by the Bradford's method. Samples were separated on a polyacrylamide gel and then transferred to a nitrocellulose membrane. After the blockage, membrane was incubated with the primary antibodies. Membrane was washed

 

with PBS and Tween 20 and incubated with secondary peroxidase-conjugated antibodies. ECL Plus Western Blotting Detection Reagents (GE Healthcare Chalfont St. Giles, UK) were used to detect bound antibodies.

### *Statistical analysis*

Comparisons between groups were performed by unpaired Student *t* test when there was a normal distribution. When data showed a non-normal distribution, comparisons between groups were made with Mann-Whitney test. The association between soleus cross-sectional fibre area and follistatin protein expression was assessed with a Spearman correlation coefficient. The level of significance was 5%.

## Results

### *General characteristics of the rats*

Clinical and pathological findings suggesting heart failure were observed in the MI group. Two animals exhibited tachypnea/dyspnoea; all rats had right ventricular hypertrophy, seven had pleural effusion, two had atrial thrombi, and two had ascites. No heart failure evidence was observed in the Sham group. Anatomical data are shown in Table 1. Body weight (BW), left ventricle weight (LVW), and LVW/BW ratio were similar between groups. Right ventricle weight (RVW), atria weight and RVW/BW and atria/BW ratios were greater in the MI than Sham group. The lung and liver wet weight-to-dry weight ratios were higher in MI than the Sham group. Soleus and gastrocnemius weight in absolute values and normalized to body weight were similar between groups.

In MI group, infarcted area was 42.9 ± 4.9% of the total left ventricle area (mean ± standard deviation).

**Table 1** Anatomical data

| | Sham ($n$ = 10) | MI ($n$ = 10) | $P$-value |
|---|---|---|---|
| BW (g) | 490 ± 50 | 469 ± 47 | 0.719 |
| LVW (g) | 0.97 ± 0.15 | 0.97 ± 0.12 | 0.937 |
| RVW (g) | 0.26 ± 0.04 | 0.57 ± 0.12 | <0.001 |
| Atria (g) | 0.10 ± 0.03 | 0.26 ± 0.10 | <0.001 |
| LVW/BW (mg/g) | 1.96 ± 0.13 | 2.07 ± 0.30 | 0.56 |
| RVW/BW (mg/g) | 0.54 ± 0.06 | 1.21 ± 0.22 | <0.001 |
| Atrium/BW (mg/g) | 0.21 ± 0.05 | 0.56 ± 0.18 | <0.001 |
| Lung wet/dry | 4.78 ± 0.21 | 5.00 ± 0.21 | 0.045 |
| Liver wet/dry | 3.02 ± 0.16 | 3.26 ± 0.16 | 0.006 |
| Soleus (g) | 0.238 ± 0.048 | 0.247 ± 0.058 | 0.72 |
| Soleus/BW (mg/g) | 0.484 ± 0.059 | 0.516 ± 0.125 | 0.48 |
| Gastrocnemius (g) | 2.76 ± 0.18 | 2.76 ± 0.21 | 0.98 |
| Gastrocnemius/BW (mg/g) | 5.67 ± 0.43 | 5.77 ± 0.47 | 0.68 |

Data are mean ± SD; Student's *t*-test.
MI, animals with myocardial infarction-induced heart failure; *n*, number of animals; BW, body weight; LVW, left ventricle weight; RVW, right ventricle weight; wet/dry, wet weight-to-dry weight ratio.

### *Echocardiographic evaluation*

Tables 2 and 3 show cardiac structure parameters and LV function data. LV diastolic and systolic diameters (LVDD and LVSD, respectively), LV diastolic posterior wall thickness, left atrium dimension (LA), LA-to-aorta diameter ratio and values of LVDD and LA normalized to body weight were significantly higher in the MI than Sham group. Aortic dimension was smaller in MI. Left ventricular diastolic septal wall thickness was similar in both groups. Heart rate was similar between groups. Endocardial fractional shortening and posterior wall shortening velocity were lower in MI. Mitral A wave was lower in MI and mitral E wave and E/A ratio were higher in MI than the Sham group. E wave deceleration time was lower in MI and isovolumetric relaxation time was not different between groups.

### *Morphological analysis*

In the soleus muscles, fibre cross-sectional areas were lower in MI than in Sham group (Sham 3572 ± 378; MI 2982 ± 323 $\mu m^2$; $P$ = 0.006). In the gastrocnemius muscle, there was no difference in fibre cross-sectional areas between

**Table 2** Echocardiographic data of cardiac structures

| | Sham ($n$ = 10) | MI ($n$ = 10) | $P$-value |
|---|---|---|---|
| LVDD (mm) | 9.14 ± 0.81 | 11.58 ± 1.64 | 0.002 |
| LVDD/BW (mm/kg) | 17.98 ± 0.62 | 23.10 ± 4.64 | 0.008 |
| LVSD (mm) | 5.21 ± 0.82 | 9.65 ± 1.48 | <0.001 |
| LVDPWT (mm) | 1.67 ± 0.12 | 1.86 ± 0.15 | 0.011 |
| LVDSWT (mm) | 1.71 ± 0.10 | 1.61 ± 0.19 | 0.24 |
| AO (mm) | 4.04 ± 0.13 | 3.68 ± 0.17 | <0.001 |
| LA (mm) | 6.16 ± 0.49 | 8.64 ± 1.13 | <0.001 |
| LA/AO | 1.53 ± 0.13 | 2.35 ± 0.31 | <0.001 |
| LA/BW (mm/kg) | 15.25 ± 0.90 | 17.21 ± 3.22 | <0.001 |

Data are mean ± SD; Student's *t*-test.
MI, animals with myocardial infarction-induced heart failure; *n*, number of animals; LVDD and LVSD, left ventricular (LV) diastolic and systolic dimension, respectively; BW, body weight; LVDPWT, LV diastolic posterior wall thickness; LVDSWT, LV diastolic septal wall thickness; AO, aorta dimension; LA, left atrium dimension.

 

**Table 3** Echocardiographic data of left ventricular function

| | Sham ($n$ = 10) | MI ($n$ = 10) | $P$-value |
|---|---|---|---|
| HR (bpm) | 270 ± 15 | 326 ± 110 | 0.18 |
| FS (%) | 43.2 ± 4.5 | 16.7 ± 5.5 | <0.001 |
| PWSV (mm/s) | 37.8 ± 5.3 | 20.2 ± 3.3 | <0.001 |
| E-wave | 84.0 ± 11.6 | 117.6 ± 16.7 | <0.001 |
| A-wave | 57.9 ± 17.5 | 23.3 ± 8.6 | <0.001 |
| E/A | 1.52 ± 0.27 | 5.78 ± 2.18 | <0.001 |
| EDT (ms) | 52.0 ± 6.0 | 31.3 ± 8.0 | <0.001 |
| IVRT (ms) | 27.3 ± 2.6 | 24.8 ± 4.1 | 0.17 |

Data are mean ± SD; Student's *t*-test.
MI, animals with myocardial infarction-induced heart failure; *n*, number of animals; HR, heart rate; bpm, beats per minute; FS, endocardial fractional shortening; PWSV, posterior wall shortening velocity; E-wave and A-wave, early and late diastolic mitral inflow, respectively; EDT, E wave deceleration time; IVRT, isovolumetric relaxation time.

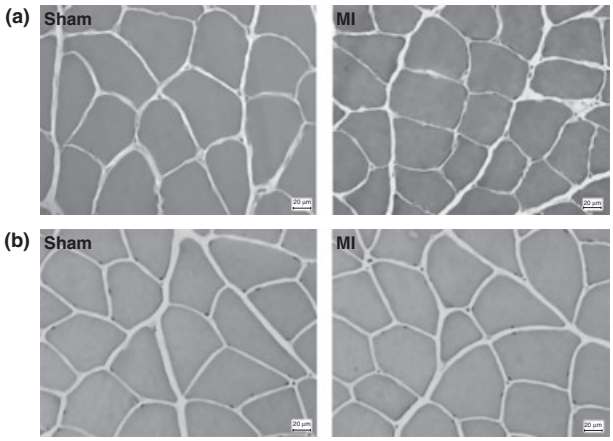


**Figure 1** Soleus (a) and gastrocnemius (b) muscles morphology; sections stained by haematoxylin and eosin. MI: rats with myocardial infarction-induced heart failure.

groups (Sham 3340 ± 443; MI 3183 ± 418; $P$ = 0.47; Figures 1 and 2).

### *Real-time RT-PCR analysis*

Myostatin gene expression was statistically similar between groups in both soleus (Sham 1.00 ± 0.34; MI 0.69 ± 0.21 arbitrary units; $P$ = 0.49) and gastrocnemius (Sham 1.00 ± 0.09; MI 1.04 ± 0.18 arbitrary units; $P$ = 0.84) muscles. There was a trend for follistatin gene expression to be lower in the MI than the Sham group in soleus muscle (Sham 1.00 ± 0.23; MI 0.48 ± 0.10 arbitrary units; $P$ = 0.085). Follistatin gene expression was not statistically

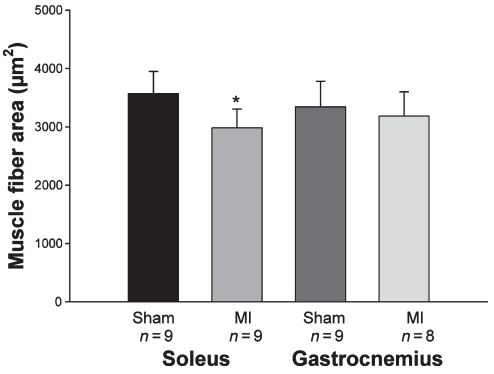


**Figure 2** Fibres cross-sectional areas of soleus and gastrocnemius muscles. MI: rats with myocardial infarction-induced heart failure. Data are expressed as mean ± SD; Student's *t*-test; *$P$ = 0.006.

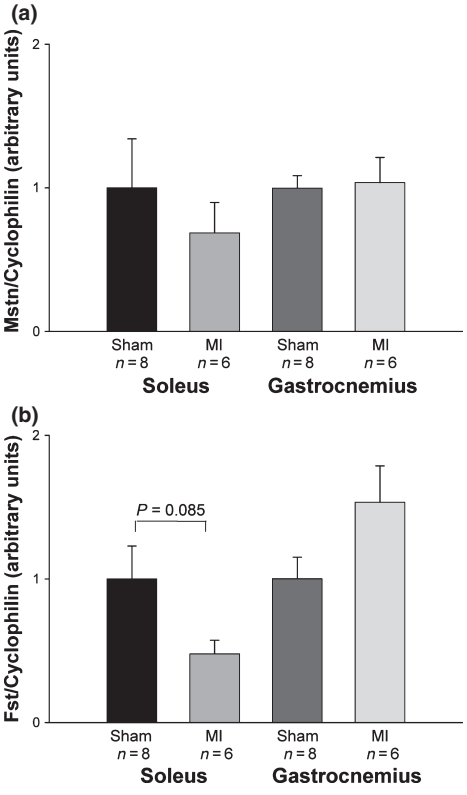


**Figure 3** Quantification of myostatin (a) and follistatin (b) mRNA gene expression in soleus and gastrocnemius muscles. MI: rats with myocardial infarction-induced heart failure. Data are expressed as mean ± SEM; Student's *t*-test.

different between groups in gastrocnemius muscle (Sham 1.00 ± 0.15; MI 1.53 ± 0.25 arbitrary units; $P$ = 0.094; Figure 3).

 

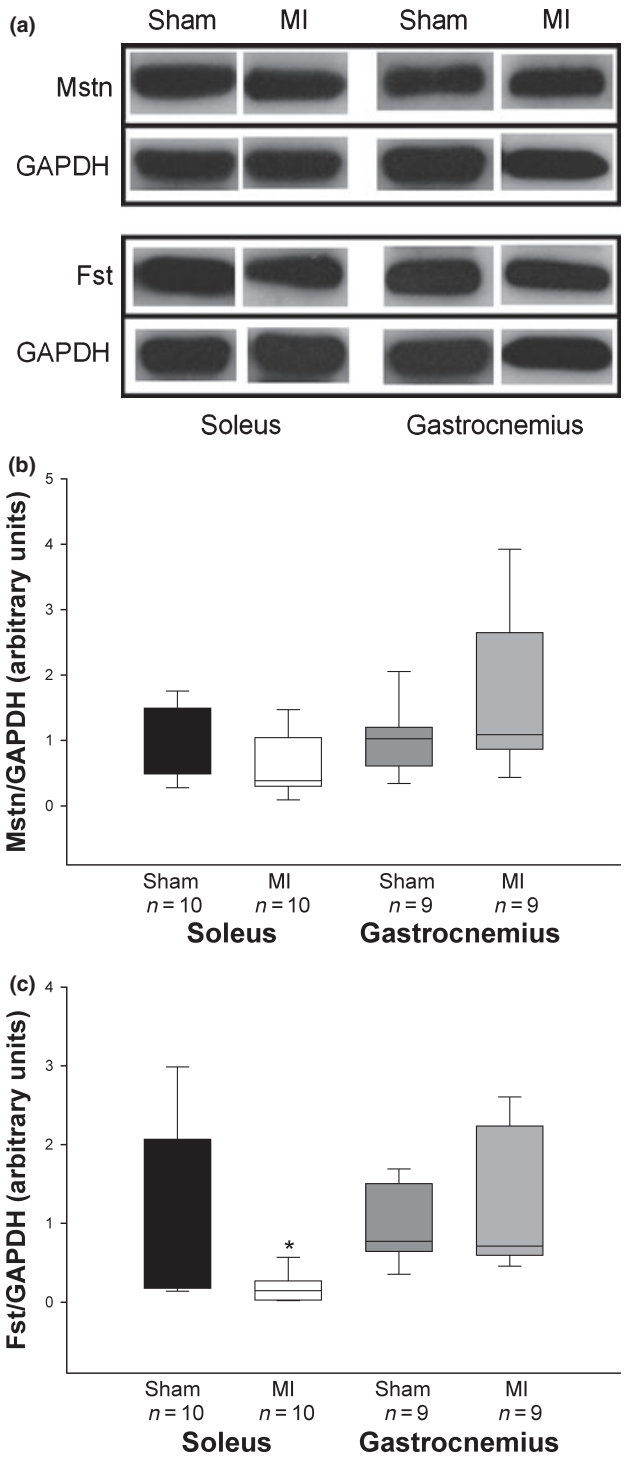


**Figure 4** (a) Representative Western blots of myostatin, follistatin, and GAPDH. Quantification of myostatin (b) and follistatin (c) protein levels in soleus and gastrocnemius muscles. MI: rats with myocardial infarction-induced heart failure. Data are expressed as median (lower quartile – upper quartile); Mann–Whitney test; $^*P = 0.03$.

*Western blotting analysis*

Myostatin protein levels were not statistically different between groups in soleus (Sham 1.00 ± 0.18; MI 0.62 ± 0.15 arbitrary units; $P = 0.12$) and gastrocnemius (Sham 1.00 ± 0.17; MI 1.66 ± 0.43 arbitrary units; $P = 0.29$) muscles. Follistatin protein expression was lower in MI than Sham in the soleus muscle (Sham 1.00 ± 0.36; MI 0.18 ± 0.06 arbitrary units; $P = 0.03$). There was no difference in follistatin protein levels between groups in the gastrocnemius muscle (Sham 1.00 ± 0.16; MI 1.21 ± 0.30 arbitrary units; $P = 0.93$; Figure 4). Follistatin protein expression in the soleus muscle showed no correlation with soleus fibre cross-sectional area ($P = 0.738$).

## Discussion

In this study, we evaluated myostatin and follistatin expression and skeletal muscle trophism in peripheral skeletal muscles of rats with myocardial infarction-induced heart failure. The new finding in this work is that decreased soleus muscle trophism was combined with unchanged myostatin expression and reduced follistatin protein levels during chronic heart failure.

The myocardial infarction model has often been used to induce experimental heart failure as it imitates frequent human cardiac failure causes such as myocardial ischemia and infarction (Pfeffer *et al.* 1979, 1992). Furthermore, the ensuing heart failure develops slowly, as usually observed in clinical settings. However, as mentioned before, only animals with a large left ventricle infarcted area evolve into heart failure. Therefore, after an early echocardiogram, we were able to exclude animals with small or moderate sized infarcts.

Heart failure diagnosis was based on pathological evidence of heart failure, which included pleuropericardial effusion, atrial thrombi, and right ventricular hypertrophy (Bing *et al.* 1995; Conrad *et al.* 1995; Brooks *et al.* 1997; Cicogna *et al.* 1999). Six months after inducing myocardial infarction, all rats with large myocardial infarction size (MI group) presented at least two of these heart failure conditions. As expected, rats from the MI group had cardiac structural alterations and left ventricular dysfunction at echocardiographical evaluation. Structural changes in the MI group included dilation of the left atrium and left ventricle, and hypertrophy of the left ventricular posterior wall. The systolic function parameters endocardial fractional shortening and posterior wall shortening velocity were highly reduced in MI group. The variables of diastolic function E-wave, A-wave, E/A ratio, and E wave deceleration time were all changed in MI.

 

In this study, we evaluated myostatin and follistatin expression in the soleus and gastrocnemius muscles. The soleus is mainly composed by type I, slow fibres, and the white gastrocnemius is mainly composed of type II, fast twitch fibres. A reduction in fibre cross-sectional area was observed in the MI group only in soleus muscle. Despite this reduced cross-sectional area, soleus muscle weight, both absolute and normalized to body weight, was not changed in the MI group. As MI group presented lung and hepatic congestion, heart failure-induced peripheral oedema may have contributed to muscle weight preservation. In gastrocnemius, muscle trophism was not changed. Although skeletal muscle atrophy has been frequently observed in experimental heart failure (Delp *et al.* 1997; Carvalho *et al.* 2003; Schulze *et al.* 2003; Dalla Libera *et al.* 2004), there are few studies specifically evaluating trophism of the gastrocnemius muscle. In rats with acute heart failure induced by interleukin-6, Janssen *et al.* (Janssen *et al.* 2005) found reduced cross-sectional fibre areas in the gastrocnemius muscle. However, Dahl rats with chronic heart failure induced by sodium overload did not present atrophy of the same muscle (Persinger *et al.* 2003). We did not find reports on the gastrocnemius trophism during myocardial infarction-induced heart failure in rats. In experimental studies, it has been observed that different skeletal muscles can be differentially affected during heart failure (De Sousa *et al.* 2002; Spangenburg *et al.* 2002).

Despite heart failure associated skeletal muscle atrophy often being described in clinical (Sullivan *et al.* 1990; Mancini *et al.* 1992; Anker & Coats 1999; Toth *et al.* 2006) and experimental (Vescovo *et al.* 1998; Carvalho *et al.* 2003; Dalla Libera *et al.* 2004) studies, the pathophysiological mechanisms are still poorly understood. As previously reported, myostatin down regulates skeletal muscle growth during embryonic and adult life (McPherron & Lee 1997; Lee 2004) and its expression is inversely associated with muscle mass in several pathological states. However, the mechanisms responsible for myostatin gene and protein expression in normal muscles are not completely understood (Lee & McPherron 2001; Lee 2004) and, in pathological situations, there are only a few clinical and experimental studies (Gonzalez-Cadavid *et al.* 1998; Siriett *et al.* 2006; Sun *et al.* 2006; Costelli *et al.* 2008; Liu *et al.* 2008; Lenk *et al.* 2009). In HIV-infected men, myostatin appears to attenuate skeletal muscle growth and contribute to muscle wasting (Gonzalez-Cadavid *et al.* 1998). Inhibition of myostatin expression leads to increased muscle growth in cancer cachectic mice (Liu *et al.* 2008) and reduces age-related sarcopenia in mice (Siriett *et al.* 2006).

Thus, in this study, we expected that reduced muscle trophism would be associated with increased myostatin expression. It was surprising to observe that myostatin mRNA and protein expression were not statistically different between Sham and MI groups in both skeletal muscles, soleus and gastrocnemius. However, we observed a trend for follistatin gene expression to be decreased in addition to reduced follistatin protein expression in MI group soleus muscle, which presented reduced fibre cross-sectional area. Myostatin activity can be modulated by physiological inhibitors and the balance between myostatin and its inhibitors is considered important in skeletal muscle mass regulation (Lee 2004). Follistatin is a potent myostatin antagonist, which can also bind to a number of other TGF-β family members (Lee 2004). Experimental studies have shown that follistatin plays an important role in modulating myostatin activity *in vivo*. Muscle mass was dramatically increased in transgenic mice overexpressing follistatin (Lee & McPherron 2001). In experimental cancer cachexia, reduced gastrocnemius weight was observed together with unchanged myostatin and reduced follistatin expression (Costelli *et al.* 2008). Thus, the results of the present study suggest that decreased follistatin expression in the soleus muscle could have increased myostatin activity and played a role in the reduced muscle trophism. It should be pointed out, however, that we failed to show a correlation between soleus fibres cross-sectional area and follistatin protein expression. It is possible that the small number of samples played a role in the lack of correlation between these variables and additional studies are necessary to clarify this topic.

Our results contrast with those from a recently published study by Lenk *et al.* (Lenk *et al.* 2009), which reported increased myostatin protein levels in the gastrocnemius muscle of rats with myocardial infarction-induced heart failure. The authors did not present data on muscle trophism. As in several pathological conditions, myostatin expression can be differentially changed according to the period of evaluation (Carlson *et al.* 1999; Baumann *et al.* 2003; Ma *et al.* 2003; Costelli *et al.* 2008), these divergent results may be due to the different observation periods after inducing myocardial infarction, 8 weeks in Lenk *et al.* study (Lenk *et al.* 2009) *vs.* 6 months in ours.

In conclusion, our data show that during chronic heart failure, decreased skeletal muscle trophism is combined with unchanged myostatin and reduced follistatin expression. Additional studies are necessary to identify molecular pathways involved in follistatin down regulation during heart failure as well as the potential role of myostatin and follistatin signalling as a new target to prevent and treat heart failure associated muscle wasting.

## Acknowledgements

The authors thank José Carlos Georgette for technical assistance and Colin Edward Knaggs for language editing. Financial support: FAPESP (Proc. n. 2006/61835-9 and 2005/60767-7), CNPq (Proc. n. 310547/2006-7 and 309494/2006-0), and Fundunesp (Proc. n. 00108/06-DFP).

## References

Acharyya S. & Gutttridge D.C. (2007) Cancer cachexia signaling pathways continue to emerge yet much still points to the proteasome. *Clin. Cancer Res.* **13**, 1356–1361.

Ahmet I., Wan R., Mattson M.P., Lakatta E.G., Talan M. (2005) Cardioprotection by intermittent fasting in rats. *Circulation* **112**, 3115–3121.

Anker S.D. & Coats A.J.S. (1999) Cardiac cachexia A syndrome with impaired survival and immune and neuroendocrine activation. *Chest* **115**, 836–847.

Baumann A.P., Ibebunjo C., Grasser W.A., Paralkar V.M. (2003) Myostatin expression in age and denervation-induced skeletal muscle atrophy. *J. Musculoskelet. Neuronal. Interact.* **3**, 8–16.

Bing O.H.L., Brooks W.W., Robinson K.G. *et al.* (1995) The spontaneously hypertensive rat as a model of the transition from compensated left ventricular hypertrophy to failure. *J. Mol. Cell. Cardiol.* **27**, 383–396.

Brooks W.W., Bing O.H.L., Robinson K.G., Slawsky M.T., Chaletsky D.M., Conrad C.H. (1997) Effect of angiotensin-converting enzyme inhibition on myocardial fibrosis and function in hypertrophied and failing myocardium from the spontaneously hypertensive rat. *Circulation* **96**, 4002–4010.

Bruera E. & Sweeney C. (2000) Cachexia and asthenia in cancer patients. *Lancet* **1**, 138–147.

Carlson C.J., Booth F.W., Gordon S.E. (1999) Skeletal muscle myostatin mRNA expression is fiber-type specific and increases during hindlimb unloading. *Am. J. Physiol.* **277**, R601–R606.

Carvalho R.F., Cicogna A.C., Campos G.E.R. *et al.* (2003) Myosin heavy chain expression and atrophy in rat skeletal muscle during transition from cardiac hypertrophy to heart failure. *Int. J. Exp. Path.* **84**, 201–206.

Cicogna A.C., Robinson K.G., Conrad C.H. *et al.* (1999) Direct effects of colchicine on myocardial function Studies in hypertrophied and failing spontaneously hypertensive rats.. *Hypertension* **33**, 60–65.

Conrad C.H., Brooks W.W., Hayes J.A., Sen S., Robinson K.G., Bing O.H.L. (1995) Myocardial fibrosis and stiffness with hypertrophy and heart failure in the spontaneously hypertensive rat. *Circulation* **91**, 161–170.

Costelli P., Muscaritoli M., Bonetto A. *et al.* (2008) Muscle myostatin signalling is enhanced in experimental cancer cachexia. *Eur. J. Clin. Invest.* **38**, 531–538.

Dalla Libera L., Ravara B., Volterrani M. *et al.* (2004) Beneficial effects of GH/IGF-I on skeletal muscle atrophy and function in \experimental heart failure. *Am. J. Physiol. Cell Physiol.* **286**, C138–C144.

De Sousa E., Lechene P., Fortin D. *et al.* (2002) Cardiac and skeletal muscle energy metabolism in heart failure: beneficial effects of voluntary activity. *Cardiovasc. Res.* **56**, 260–268.

Delp M.D., Duan C., Mattson J.P., Musch T.I. (1997) Changes in skeletal muscle biochemistry and histology relative to fiber type in rats with heart failure. *J. Appl. Physiol.* **83**, 1291–1299.

Gonzalez-Cadavid N.F., Taylor W.E., Yarasheski K. *et al.* (1998) Organization of the human myostatin gene and expression in healthy men and HIV-infected men with muscle wasting. *Proc. Natl Acad. Sci. USA* **95**, 14938–14943.

Harrington D., Anker S.D. & Coats A.J.S. (2001) Preservation of exercise capacity and lack of peripheral changes in asymptomatic patients with severely impaired left ventricular function. *Eur. Heart J.* **22**, 392–399.

Janssen S.P., Gayan-Ramirez G., Van den Bergh A. *et al.* (2005) Interleukin-6 causes myocardial failure and skeletal muscle atrophy in rats. *Circulation* **111**, 996–1005.

Lee S.-J. (2004) Regulation of muscle mass by myostatin. *Annu. Rev. Cell. Dev. Biol.* **20**, 61–86.

Lee S.-J. & McPherron A.C. (2001) Regulation of myostatin activity and muscle growth. *Proc. Natl Acad. Sci. USA* **98**, 9306–9311.

Lenk K., Schur R., Linke A. *et al.* (2009) Impact of exercise training on myostatin expression in the myocardium and skeletal muscle in a chronic heart failure model. *Eur. J. Heart Fail.* **11**, 342–348.

Litwin S.E., Katz S.E., Weinberg E.O., Lorell B.H., Aurigemma G.P., Douglas P.S. (1995) Serial echocardiographic-doppler assessment of left ventricular geometry and function in rats with pressure-overload hypertrophy Chronic angiotensin-converting enzyme inhibition attenuates the transition to heart failure. *Circulation* **91**, 2642–2654.

Liu C.-M., Yang Z., Liu C.-W. *et al.* (2008) Myostatin antisense RNA-mediated muscle growth in normal and cancer cachexia mice. *Gene Ther.* **15**, 155–160.

Lopes F.S., Carvalho R.F., Campos G.E.R. *et al.* (2008) Down-regulation of MyoD gene expression in rat diaphragm muscle with heart failure. *Int. J. Exp. Path.* **89**, 216–222.

Ma K., Mallidis C., Bhasin S. *et al.* (2003) Glucocorticoid-induced skeletal muscle atrophy is associated with upregulation of myostatin gene expression. *Am. J. Physiol. Endocrinol. Metab.* **285**, E363–E371.

Mancini D.M., Walter G., Reichek N. *et al.* (1992) Contribution of skeletal muscle atrophy to exercise intolerance and

 

altered muscle metabolism in heart failure. *Circulation* **85**, 1364–1373.

McPherron A.C. & Lee S.-J. (1997) Double muscling in cattle due to mutations in the myostatin gene. *Proc. Natl Acad. Sci. USA* **94**, 12457–12461.

McPherron A.C., Lawler A.M., Lee S.-J. (1997) Regulation of skeletal muscle mass in mice by a new TGF-beta superfamily member. *Nature* **387**, 83–90.

Minicucci M.F., Azevedo P.S., Duarte D.R. *et al.* (2007) Comparison of different methods to measure experimenal chronic infarction size in the rat model. *Arq. Bras. Cardiol.* **89**, 83–87.

Oh B.-H., Ono S., Rockman H.R., Ross J. (1993) Myocardial hypertrophy in the ischemic zone induced by exercise in rats after coronary reperfusion. *Circulation* **87**, 598–607.

Okoshi K., Matsubara L.S., Okoshi M.P. *et al.* (2002) Food restriction-induced myocardial dysfunction demonstrated by the combination of in vivo and in vitro studies. *Nutr. Res.* **22**, 1353–1364.

Paiva S.A.R., Zornoff L.A.M., Okoshi M.P. *et al.* (2003) Ventricular remodeling induced by retinoic acid supplementation in adult rats. *Am. J. Physiol. Heart Circ. Physiol.* **284**, H2242–H2246.

Persinger R., Janssen-Heininger Y., Wing S.S., Matthews D.E., LeWinter M.M., Toth M.J. (2003) Effect of heart failure on the regulation of skeletal muscle protein synthesis, breakdown, and apoptosis. *Am. J. Physiol. Endocrinol. Metab.* **284**, E1001–E1008.

Pfeffer M.A., Pfeffer J.M., Fishbein M.C. *et al.* (1979) Myocardial infarct size and ventricular function in rats. *Circ. Res.* **44**, 503–512.

Pfeffer M.A., Braunwald E., Moye L.A. *et al.* (1992) Effect of captopril on mortality and morbidity in patients with left ventricular dysfunction after acute myocardial infarction: results of the survival and ventricular enlargement trial The SAVE Investigators. *N. Engl. J. Med.* **327**, 669–677.

Sahn D.J., DeMaria A., Kisslo J., Weyman A. (1978) Recommendations regarding quantitation in M-mode echocardiography: results of a survey of echocardiographic measurements. *Circulation* **58**, 1072–1083.

Schulze P.C., Gielen S., Adams V. *et al.* (2003) Muscular levels of proinflammatory cytokines correlate with a reduced expression of insulin-like growth factor-1 in chronic heart failure. *Basic Res. Cardiol.* **98**, 267–274.

Siriett V., Platt L., Salerno M.S., Ling N., Kambadur R., Sharma M. (2006) Prolonged absence of myostatin reduces sarcopenia. *J. Cell. Physiol.* **209**, 866–873.

Solomon S.D., Greaves S.C., Ryan M., Finn P., Pfeffer M.A., Pfeffer J.M. (1999) Temporal dissociation of left ventricular function and remodeling following experimental myocardial infarction in rats. *J. Card. Fail.* **5**, 213–223.

Spangenburg E.E., Talmadge R.J., Musch T.I., Pfeifer P.C., McAllister R.M., Williams J.H. (2002) Changes in skeletal muscle myosin heavy chain isoform content during congestive heart failure. *Eur. J. Appl. Physiol.* **87**, 182–186.

Sullivan M.J., Green H.J., Cobb F.R. (1990) Skeletal muscle biochemistry and histology in ambulatory patients with long-term heart failure. *Circulation* **81**, 518–527.

Sun D.F., Chen Y., Rabkin R. (2006) Work-induced changes in skeletal muscle IGF-1 and myostatin gene expression in uremia. *Kidney Int.* **70**, 453–459.

Toth M.J., Ades P.A., Tischler M.D., Tracy R.P., LeWinter M.M. (2006) Immune activation is associated with reduced skeletal muscle mass and physical function in chronic heart failure. *Int. J. Cardiol.* **109**, 179–187.

Vescovo G., Ceconi C., Bernocchi P. *et al.* (1998) Skeletal muscle myosin heavy chain expression in rats with monocrotaline-induced cardiac hypertrophy and failure. Relation to blood flow and degree of muscle atrophy. *Cardiovasc. Res.* **39**, 233–241.

Whittemore L.-A., Song K., Li X. *et al.* (2003) Inhibition of myostatin in adult mice increases skeletal muscle mass and strength. *Biochem. Biophys. Res. Commun.* **291**, 701–706.

Zimmers T.A., Davies M.V., Koniaris L.G. *et al.* (2002) Induction of cachexia in mice by systemically administered myostatin. *Science* **296**, 1486–1488.

Zornoff L.A.M., Matsubara B.B., Matsubara L.S., Paiva S.A.R., Spadaro J. (2000) Early rather than delayed administration of lisinopril protects the heart after myocardial infarction in rats. *Basic Res. Cardiol.* **95**, 208–214.

 